THERMAL TEMPERATURE IN AVALANCHE FLOW

Cesar Vera Valero, Thomas Feistl, Walter Steinkogler, Othmar Buser and Perry Bartelt*
WSL Institute for Snow and Avalanche Research SLF, Davos, Switzerland

ABSTRACT: The thermal temperature of snow greatly influences the flow behaviour of avalanches. It is even common to implicitly characterize avalanche flow with respect to the thermal regime: "wet" snow avalanches contain warm, moist snow whereas "dry" flowing or powder avalanches consist of colder snow, below the melting point of ice. Despite its importance, thermal effects are largely neglected in avalanche dynamics calculations. In this contribution we explicitly calculate the avalanche flow temperature by considering two irreversible thermodynamic processes: (1) the shear work operating on the mean kinetic energy of the avalanche and (2) the dissipation of fluctuation energy due to random granular interactions. These energy fluxes regulate the configurational energy of the avalanche and therefore the flow form. However, a third, and perhaps more important source of thermal energy, is from snow entrainment. We model the temperature evolution of an avalanche by extending the basic set of differential equations used to simulate avalanches with snow energy entrainment in real terrain. Using an avalanche event at the Vallée de la Sionne test site, we show that the temperature of the snow in the starting zone in relation to the temperature of the snowcover encountered by the avalanche at lower elevations determines the thermal flow regime and therefore the behaviour of the avalanche in the runout zone. The inclusion of snow granule properties in flow models is essential to understand how temperature influences avalanche behaviour. Higher temperatures increase the dissipation of fluctuation energy of the random granular interactions – but decrease the shear work because of lubrication. This competition between the two primary irreversible processes in avalanches results in a wide range of flow behaviour, flow forms and depositional structures.

1. INTRODUCTION

Avalanche dynamics calculations are usually carried out without consideration of the thermal temperature. This is somewhat surprising considering that the mechanical behavior of snow -- including avalanching snow in the form of snowcover fragments, granules and powder dust-- is greatly influenced by temperature. For example, the flow behavior of a moist wet snow (warm) avalanche differs greatly from a dry powder (cold) avalanche. Although the runout might be the same, the speed, the flow configuration (flowing, powder) and the structure of the avalanche deposits (granule size, levees, flow fingers) will differ greatly. Another indication that temperature plays an important role in avalanche dynamics calculations is the fact that melt planes are often found in avalanche deposits, suggesting immense frictional heating and the possibility of some meltwater lubrication.

* *Corresponding author address:* Perry Bartelt, WSL Institute for Snow and Avalanche Research, CH-7260 Davos, Switzerland; tel: (+41) 81 - 4170251; fax: (+41) 81- 4170110; email: bartelt@slf.ch.

If any consideration of the temperature does come into play, it is usually by modifying the friction parameters, adjusting them to model the desired runout and velocity of the observed event. In practice, since extreme runout and velocity are required in a hazard analysis, the temperature enters the calculation implicitly in the choice of the extreme friction parameters.

In this paper, we will explicitly calculate the evolution of thermal temperature during avalanche motion. We account for both laminar and turbulent dissipative energy fluxes that raise the internal heat energy of the avalanche (Bartelt et al., 2006). Our results indicate that the dissipation of the turbulent energy flux is responsible for the flow form of the avalanche. Since the granule properties are strongly related to the decay of the turbulent kinetic energy, this result suggests that the temperature strongly influences the granule properties (Bartelt and McArdell, 2009). However, our most important result is that the temperature of the entrained snow essentially determines the temperature regime of the avalanche, despite the inclusion of frictional heating. The practical consequence of this result is that warning services should be aware of both the snow temperature and distribution of snow to predict extreme avalanche runout and behavior.

2. MODEL EQUATIONS

In the **RAMMS** (Christen et al., 2010a, Bartelt et al, 2012) model the mathematical description of the mountain terrain is defined in a horizontal $X-Y$ coordinate system with a given resolution, typically given by the resolution of aerial laser scanning. The elevation $Z(X,Y)$ is specified for each coordinate pair (Buehler et al., 2011). A local (x,y,z) coordinate system is introduced with directions x and y parallel to the geographic coordinates X and Y. The gravitational acceleration is decomposed into three components for each element

$$g = g_x\mathbf{i} + g_y\mathbf{j} + g_z\mathbf{k}\,. \tag{1}$$

We define the velocity, shear and gravity vectors

$$\mathbf{V} \equiv u\mathbf{i} + v\mathbf{j} \tag{2}$$

$$\mathbf{S} \equiv S_x\mathbf{i} + S_y\mathbf{j} \tag{3}$$

$$\mathbf{G} \equiv mg_x\mathbf{i} + mg_y\mathbf{j} \tag{4}$$

where m is the mass per unit area. Using the substantial derivative operator

$$\frac{d}{dt}(\cdots) = \frac{\partial}{\partial t}(\cdots) + (\mathbf{V}\cdot\nabla)(\cdots) \tag{5}$$

we solve the following differential equations governing mass and momentum balances

$$\frac{dm}{dt} = Q_e \tag{6}$$

$$m\frac{d\mathbf{V}}{dt} + \nabla(mg_z) = \mathbf{G} - \mathbf{S} \tag{7}$$

with the additional equations governing the fluctuation energy R and internal heat energy e:

$$\frac{dR}{dt} = \alpha(\mathbf{S}\cdot\mathbf{V}) - \beta R \tag{8}$$

$$\frac{de}{dt} = (1-\alpha)(\mathbf{S}\cdot\mathbf{V}) + \beta R + E\,. \tag{9}$$

The fluctuation parameters α and β (Buser and Bartelt, 2009) govern the increase of granular turbulence (random fluctuation energy) from the mean shear work (parameter α) and the dissipation of fluctuation energy to heat by various processes such as inelastic collisions, plastic deformations or abrasive rubbing (parameter β).

The vector products

$$\dot{W}_g = \mathbf{G}\cdot\mathbf{V} \quad \text{and} \quad \dot{W}_f = \mathbf{S}\cdot\mathbf{V} \tag{10}$$

define the gravitational and frictional work rates. Note that the splitting Eqs 8 and 9 is such that

$$\frac{dR}{dt} + \frac{de}{dt} = \dot{W}_f \tag{11}$$

ensuring that all fluctuation energy is dissipated to heat and the governing equations are energy conserving.

The only undefined quantities in the model equations are the snowcover mass entrainment rate Q_e and the associated energy entrainment rate E:

$$E = cQ_eT_e \tag{12}$$

which depends on the thermal temperature of the snowcover T_e. The quantity c is the specific heat of snow. The change in mean thermal temperature is thus controlled by three energy fluxes: the part of the shear work that is immediately transformed to heat $(1-\alpha)(\mathbf{S}\cdot\mathbf{V})$; the rise due to the dissipation of fluctuation energy βR and the change due to mass entrainment E. The first two energy fluxes will always cause an increase in temperature, whereas the entrainment of low temperature snow mass can cause a decrease in flow temperature.

The mean flow density ρ is defined with respect to the granule density γ and the solid volume fraction η

$$\rho \equiv \gamma\eta = \frac{m}{h}. \qquad (13)$$

The flow height h accounts for volume changes induced by dispersive pressures arising from the granular interactions with the ground, see Buser and Bartelt (2011). The density is not constant during the flow and is defined by the configurational energy of the avalanche. To model avalanche fricition, we apply a standard Voellmy model (Voellmy, 1955, Salm 1993) modified by the fluctuation energy (Christen et al., 2010a, Christen et al., 2010b)

$$S = \mu(R)N + \frac{\rho g \|U\|^2}{\xi(R)}. \qquad (14)$$

The functional dependency of the friction coefficients on the fluctuation energy is discussed in Bartelt et al. (2012).

3. RESULTS

On February 7th, 2003 a mixed flowing powder avalanche (VdlS No. 509) was artificially released by explosives from the Creta Bess 1 release zone of the Vallée de la Sionne test site (Figure 1). The release zone was large (55'000 m2), but as the avalanche occurred after an extensive period of avalanching (VdlS Nos. 504 and 506 on the 31st of January, see Christen et al., 2010 and VdlS No. 5274) much of the snowcover had already been entrained by earlier avalanches. We specified in accordance with the measured snowcover heights before the avalanche of 0.2 m. The starting mass was 11,500 tons of snow.

We first simulated the avalanche, back-calculating the flow velocity and runout distance. The avalanche ran-up the counter slope and covered the observation bunker. We selected the following parameters μ = 0.57 (static friction angle of snow), ξ = 2000 m/s^2 (turbulent Reynold's stresses), α = 0.06 (turbulent kinetic energy flux, production, roughness), β = 0.8 1/s (turbulent kinetic energy, decay, moist snow). The simulation matched the measured velocity distribution (maximum velocity 52 m/s) and runout distance.

To calculate how the temperature change during the avalanche motion, we specified that the initial temperature of the release mass to be T = -10°C We then performed three simulations with different snow cover temperatures: T_e = 0°C, T_e = -5°C and T_e = -10°C .

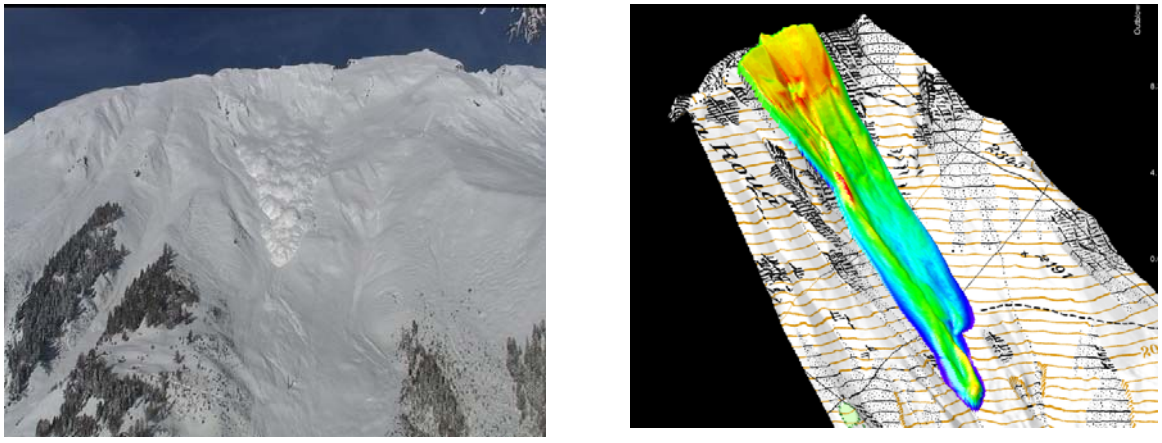

Fig 1. VdlS avalanche No. 509 of February 7th, 2003. Numerical simulation with **RAMMS** model showing the calculated heights of suspension layer. Observed and calculated plume heights at the front of the avalanche are approximately 20 m. The avalanche is moving at 50 m/s. The numerical model does not account for the lateral spreading of the cloud after blow-out.

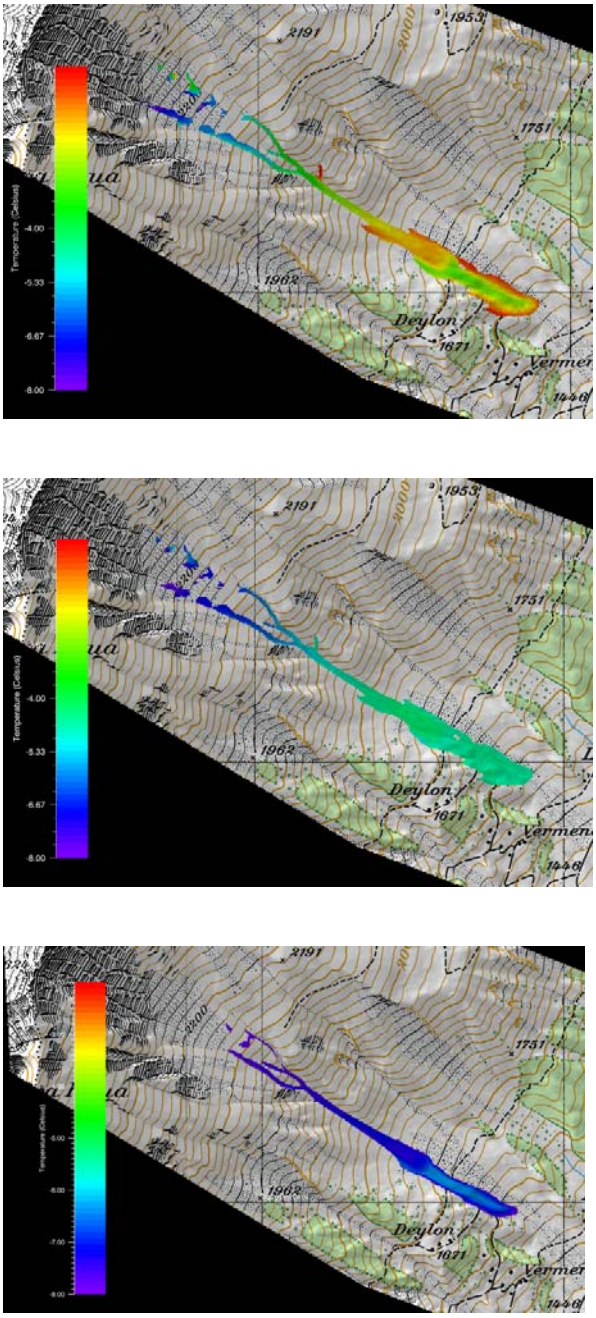

Fig. 2: Temperature distribution in the flowing avalanche as it passes the mast. Top: T_e = 0 °C. Middle: T_e = -5 °C. Bottom: T_e = -10 °C . The largest temperature gradients are when the avalanche entrains 0 °C snow.

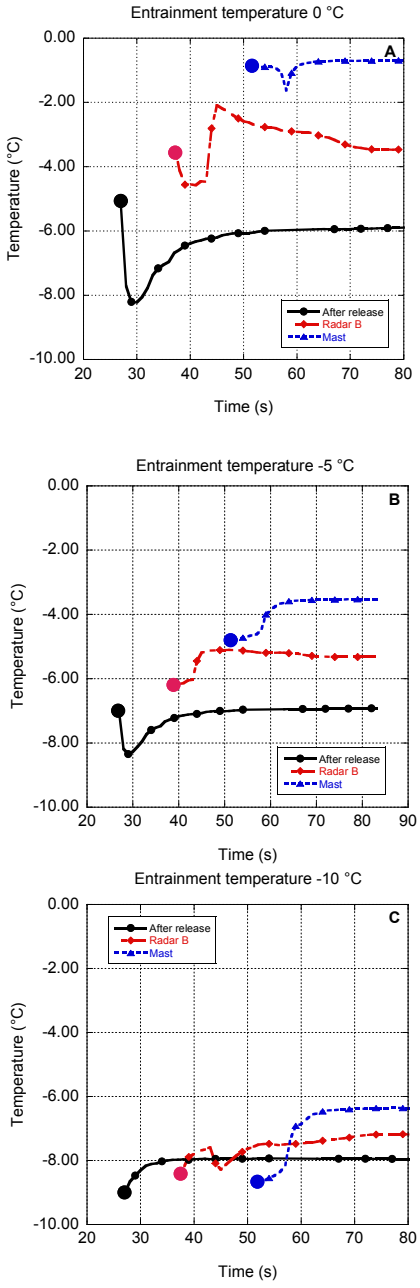

Fig. 3: Mean avalanche temperature at different flow positions (after release, radar B and mast) for different entrainment temperatures. A: T_e = 0°C, B: T_e = -5°C and C: T_e = -10°C . Starting temperature of the avalanche T = -10°C . The temperature barely increases when entraining T = -10°C snow.

The calculated avalanche temperatures are depicted in Figure 2 and Figure 3. The avalanche temperature increases the most when it entrains warm snow (Figure 2A and Figure 3A). When the snowcover has the same temperature as the release zone, the rise in temperature is small. We calculated the heating rates as the avalanche front passed over three different locations. The largest rates occurred when the avalanche entrained T_e = 0 °C snow (approximately 0.15 °C/s, see Table 1) and lowest for the T_e = -10 °C snowcover case (approximately zero, see Table 1).

	Radar B	Mast
Entrainment 0°C	0.16 °C/s	0.17 °C/s
Entrainment - 5°C	0.11 °C/s	0.08 °C/s
Entrainment -10°C	0.04 °C/s	- 0.01 °C/s

Table 1: Change in avalanche front temperature between release and radar B and between radar B and Mast. The largest temperature increases are when the entrainment temperature is T_e = 0 °C.

We also found that the lateral temperature within the avalanche varied greatly depending on the snowcover temperature. When warm snow is entrained at the extremities of the avalanche (front and sides), the temperature is warmer than in the flowing core, if the release temperature is low (Figure 4A). A relatively flat, homogeneous profile is obtained when the entrained snow has the approximate temperature the avalanche has attained by frictional heating (Figure 4B). For the case, where the temperature is low, the entrained snow cools the avalanche front and sides (Figure 4C). Thus, the lateral temperature gradients in the avalanche are an indication of the initial temperature distribution between the release and runout zones.

It is possible to predict when and where phase changes occur within the flowing avalanche. Meltwater lubrication is often cited as a physical driver of enhanced avalanche runout. We have noted refrozen melt planes in the deposits as well on granule surfaces (Bartelt and McArdell, 2009). This too depends on the distribution of temperature between the release zone and runout and the amount of entrained snow. We set the starting zone temperature to T = -7 °C and let the avalanche entrain warm snow at T_e = -1°C. The location of the meltzone is depicted in Figure 5. The maximum amount of water production was on the order of 0.15 mm/m^2 which is enough to produce a water film thickness of several micro-meters.

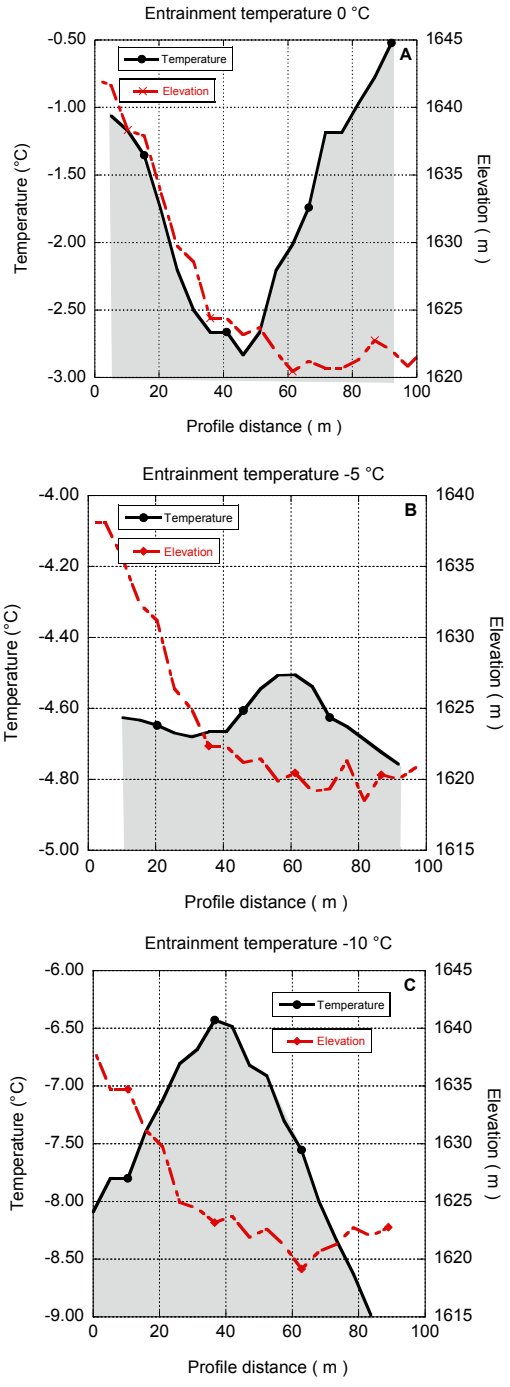

Fig. 4. Calculated lateral temperature profiles at the measurement mast for three different entrainment temperatures: A: T_e = 0 °C, B: T_e = -5 °C and C: T_e = -10 °C .

4. CONCLUSIONS

We extended the governing differential equations of avalanche flow to include the calculation of the avalanche temperature from initiation to runout. Although this is the mean, depth-averaged temperature, we found that snow entrainment determines the temperature regime of the avalanche. Heating by friction exists; however, the temperature change is primarily controlled by the temperature of the snowcover. Therefore, it is not only mass entrainment that controls the flow regime and form of the avalanche (Bartelt et al, 2012), but also energy entrainment.

In our mathematical model it is important to include energy fluxes arising from the laminar and turbulent motion of the granules. The speed of the avalanche is determined not only by the laminar friction parameters but also the decay of the turbulent kinetic energy. This decay appears to be controlled by the temperature of the granules, as higher temperature snow can dissipate more energy under collisional and plastic deformations.

The inclusion of the thermal temperature in avalanche dynamics calculations appears to be a necessary step in order to create models that consider the material properties of snow on the dynamics of avalanche motion. Our results are based on the assumption of ideal mixing and depth-averaged temperatures. This is clearly not the case. In future it will therefore be essential to measure thermal temperature during the flow. This could be performed with infrared cameras as well as thermal sensors on the mast.

Fig. 5: Location of melting areas in the runout zone. Release temperature: T_e = -1 °C. Starting temperature of the avalanche T = -7 °C . Amount of water 0.15 mm/m^2.

5. REFERENCES

Bartelt, P., Buehler, Y., Buser, O., 2012. Modeling mass-dependent flow regime transitions to predict the stopping and depositional behavior of snow avalanches. Journal of Geophysical Research-earth Surface, 117, F01015 DOI:10.1029/2010JF001957

Bartelt, P., Buser, O., Platzer, K., 2006. Fluctuation-dissipation relations for granular snow avalanches. Journal of Glaciology, 52 (179) 631-643 DOI:10.3189/172756506781828476

Bartelt, P., McArdell, B. W., 2009. Granulometric investigations of snow avalanches.Journal of Glaciology, 55 (193) 829-833

Buehler, Y., Christen, M., Kowalski, J., 2011. Sensitivity of snow avalanche simulations to digital elevation model quality and resolution. Annals of Glaciology, 52 (58) 72-80

Buser, O., Bartelt, P., 2009. Production and decay of random kinetic energy in granular snow avalanches. Journal of Glaciology, 55 (189) 3-12

Buser, O., Bartelt, P., 2011. Dispersive pressure and density variations in snow avalanches. Journal of Glaciology 57 (205) 857-860

Christen, M., Kowalski, J., Bartelt, P., 2010a. RAMMS: Numerical simulation of dense snow avalanches in three-dimensional terrain. Cold Regions Science and Technology, 63 (1-2) 1-14. DOI:10.1016/j.coldregions.2010.04.005

Christen, M., Bartelt, P., Kowalski, J., 2010b. Back calculation of the In den Arelen avalanche with RAMMS: interpretation of model results. Annals of Glaciology, 51(54), 161–168.

Salm, B., 1993. Flow, flow transition and runout distances of flowing avalanches. Annals of Glaciology, 18, 221–226.

Voellmy, A., 1955. Über die Zerstörungskraft von Lawinen. Schweizerische Bauzeitung 73, 159-162, 212-217, 246-249, 280-285.